Synthesis and Crystal Structure of NaNb₂AsO₈

William T. A. Harrison,*,1 Cheryl S. Liang,† Tina M. Nenoff,‡ and Galen D. Stucky†

*Department of Chemistry, University of Houston, Houston, Texas 77204-5641; †Department of Chemistry, University of California, Santa Barbara, California 93106-9510; and ‡Sandia National Laboratories, P.O. Box 5800, MS 0709, Albuquerque, New Mexico 87185-0709

The high-temperature/high-pressure hydrothermal synthesis and X-ray single crystal structure of $NaNb_2AsO_8$ are reported. The title compound contains a three-dimensional network of NbO_6, NbO_5, and AsO_4 groups, enclosing one-dimensional channels containing seven-coordinate guest sodium cations. UV/visible measurements on $NaNb_2AsO_8$ indicate two distinct absorption features at ~285 and ~360 nm. Crystal data for $NaNb_2AsO_8$: $M_r = 410.79$, monoclinic, $P2_1/n$ (No. 14), $a = 4.8970(6)$ Å, $b = 8.516(2)$ Å, $c = 15.075(3)$ Å, $\beta = 98.971(6)°$, $V = 620.98$ Å³, $Z = 4$, $R = 5.31\%$, $R_w = 5.15\%$, 2121 observed reflections ($I > 3\sigma(I)$). © 1994 Academic Press, Inc.

INTRODUCTION

The synthesis and characterization of new materials with useful nonlinear optical (NLO) properties is an active area of research in solid-state chemistry and physics. One outstanding example of a large family of phases with technologically useful optical properties is provided by potassium titanyl phosphate ($KTiOPO_4$; KTP) and its many isotypes (1, 2). It has been suggested (3) that materials containing octahedral TiO_6 and NbO_6 groups are likely to have favorably large NLO coefficients due to their propensity to form distorted TiO_6 and NbO_6 octahedra containing short ($d < 1.8$ Å), polarizable Ti–O and Nb–O bonds, respectively. These short bonds are often referred to as titanyl Ti=O and niobyl Nb=O "double" bonds (1), although the analogy with organic C=C double bonds is not exact, and the hybridization scheme for Ti or Nb atoms (4) is quite different to those which define carbon-like σ and π bonds. However, for any *bulk* second-harmonic-generation (SHG) response to be observable, these distorted TiO_6 or NbO_6 moieties must crystallize as parts of noncentrosymmetric crystal structures. The only method available at the present time for incorporating these "favored" TiO_6 and NbO_6 groups into new types of noncentrosymmetric crystal structures with potentially useful SHG properties is via exploratory synthesis techniques.

For example, we have recently reported the syntheses, structures, and optical and spectroscopic properties of several members of a family of phases of general formula $M(Nb/Ta)_2PO_8$ (M = Li, Na, K, Ag, ...) whose structures (5, 6, 7) are based on a microporous, 3-dimensional, anionic, octahedral/tetrahedral framework containing the ion-exchangeable guest cations. These materials have powder nonlinear optical coefficients (~100 × that of quartz) comparable to that of the commercially useful β-BaB_2O_4 (8).

Because arsenic-containing isotypes of $KTiOPO_4$, such as $KTiOAsO_4$ (9), show great promise as SHG materials, we have carried out exploratory hydrothermal syntheses of sodium/niobium/arsenic-containing materials, to determine if arsenic-containing congeners of the $M(Nb/Ta)_2PO_8$-type phases can be prepared. The new phase $NaNb_2AsO_8$ was successfully synthesized in single-crystal form: However, its structure is completely different to those of the $M(Nb/Ta)_2PO_8$ family of phases and is described below. We also report X-ray powder data, ion-exchange reactions, and UV/visible spectroscopic results for $NaNb_2AsO_8$.

$NaNb_2AsO_8$ complements the large number of alkali-metal niobium phosphates and arsenates which have been structurally characterized recently, including the following phases: $CsNbOP_2O_7$ (10), $KNbOP_2O_7$ (11), $KNb_3P_3O_{15}$ (12), $K_7Nb_{14.13}P_{8.87}O_{60}$ (13), $K_3Nb_6P_4O_{26}$ (14), $Na_4Nb_8P_6O_{35}$ (15), $K_4Nb_8P_5O_{34}$ (16), $CsNb_3P_3O_{15}$ (17), $RbNb_3O_3(PO_4)_3$ (18), $K_2Na_{1.73}Nb_8P_5O_{34}$ (19), $Na_6Nb_8P_2O_{29} \cdot P_3O_6$ (20), $Na_{0.5}Nb_2(PO_4)_3$ (21), $K_2Nb_2As_2O_{11}$ (22), KNb_4AsO_{13} (23), and $K_3NbAs_2O_9$ (24). Most of these $M/Nb/P/O$ materials are related to tungsten–bronze-type structures. The relationship between the structures of the three distinct $K/Nb/As/O$ phases and that of $NaNb_2AsO_8$ is briefly described below.

SYNTHESIS AND PHYSICAL CHARACTERIZATION

The title compound was prepared by a high-temperature/high-pressure hydrothermal reaction: 2 mmol of $Na_2HAsO_4 \cdot 7H_2O$ (0.624 g), 0.4 mmol of Nb_2O_5 (0.106 g), and 2 mmol of 4 M H_3AsO_4 (0.5 ml) were sealed in a gold

tube, heated to 750°C, and held at that temperature for 60 hr in a Leco TemPres hydrothermal bomb ($P_{max} \approx$ 32,000 psi). The bomb was cooled to 400°C over a 30-h period and then turned off to cool to ambient overnight. After breaking open the gold tube, numerous rod- and needle-like crystals (yield 0.164 g) were recovered from the pH 4 mother liquor by vacuum filtration and rinsing with water. As-synthesized crystals of $NaNb_2AsO_8$ are light gold in color and have a maximum linear dimension of ~2 mm.

X-ray powder data (Scintag automated PAD-X diffractometer, θ–θ geometry, flat-plate sample, $CuK\alpha$ radiation, $\bar{\lambda} = 1.54178$ Å, $T = 25(2)°C$) were collected for a thoroughly ground sample of $NaNb_2AsO_8$. The resulting diffractogram did not match the powder patterns of any known Na/Nb/As/O phases nor those of the starting materials. The instrumental $K\alpha_1/K\alpha_2$ profile was reduced to a single $CuK\alpha_1$ peak ($\lambda = 1.540568$ Å) by a software "stripping" routine, and d-spacings were established, using silicon powder ($a = 5.43035$ Å) as an internal standard, relative to this wavelength. Peak assignments were

made on the basis of LAZY-PULVERIX (25) simulations using the single-crystal lattice parameters described below. Optimized cell parameters (with e.s.d. in parentheses) of $a = 4.892(2)$ Å, $b = 8.504(3)$ Å, $c = 15.059(5)$ Å, and $\beta = 98.96(2)°$ resulted from the monoclinic lattice-parameter refinement. No other lines were observable in the X-ray powder data. X-ray powder data for $NaNb_2AsO_8$ are reported in Table 1.

Ion exchange (molten $AgNO_3$, 225°C, 1 day) was attempted on the $NaNb_2AsO_8$ crystals. A powder pattern of the recovered, post-ion-exchange material indicated that sharply crystalline lines due to the possible $Na_{1-x}Ag_xNb_2AsO_8$ structure were present. However, many other unidentified lines, possibly due to insoluble decomposition products of $AgNO_3 + NaNb_2AsO_8$, were also visible. It was not possible to unambiguously assign Miller indices to enough reflections in the $Na_{1-x}Ag_xNb_2AsO_8$ pattern for reliable least-squares refinement and hence systematically determine if any change in unit-cell dimensions had occurred due to the ion-exchange process.

UV/visible data for ground crystals of $NaNb_2AsO_8$ were collected on a Cary 14 automated spectrometer. The resulting spectrum is illustrated in Fig. 1 and shows two distinct features, centered at ~285 and ~360 nm. The first of these we ascribe to a ligand to metal charge-transfer (LMCT) band centered on the AsO_4 group, as was observed in earlier studies of alkaline-earth arsenates (26). The 360-nm band may be attributed to a NbO_6-centered LMCT transition; a very similar feature was observed in the UV/visible spectrum of $K_{2/3}Li_{1/3}Nb_2PO_8$ (5).

Structure Determination

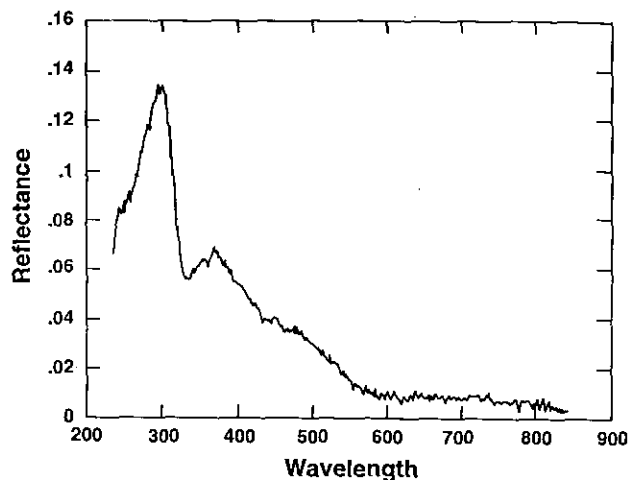The structure of $NaNb_2AsO_8$ was determined by standard single-crystal X-ray methods. A suitable single crys-

TABLE 1
X-Ray Powder Data for $NaNb_2AsO_8$

h	k	l	$2\theta_{obs}$	$\Delta(2\theta)^a$	d_{calc}	$\Delta(d)^b$	I_{rel}
0	1	1	12.049	0.013	7.383	−0.008	73
0	2	0	20.940	0.008	4.252	−0.002	17
0	2	1	21.763	−0.015	4.088	0.003	3
1	0	−3	23.657	−0.004	3.766	0.001	2
1	1	−3	25.906	−0.003	3.444	0.000	25
1	0	3	27.750	0.001	3.219	0.000	31
1	2	−1	28.009	−0.003	3.189	0.000	35
1	2	−2	29.340	0.018	3.049	−0.002	6
1	1	−4	29.868	−0.017	2.993	0.002	4
0	2	4	32.010	0.006	2.799	−0.001	100
1	0	−5	32.850	0.018	2.730	−0.001	8
0	3	2	33.870	0.000	2.649	0.000	15
1	2	3	35.010	0.020	2.566	−0.001	7
0	3	3	36.570	0.031	2.461	−0.002	3
0	2	5	36.853	−0.048	2.438	0.003	5
0	1	6	37.800	−0.024	2.380	0.001	2
2	1	0	38.760	−0.011	2.324	0.001	3
0	4	0	42.534	−0.008	2.126	0.000	2
2	1	−4	42.690	−0.007	2.119	0.000	3
1	1	−7	45.150	0.001	2.009	0.000	4
1	3	−5	46.170	−0.008	1.967	0.000	3
2	2	2	46.500	−0.004	1.953	0.000	8
2	2	−4	46.727	0.016	1.945	−0.001	6
0	0	8	49.020	0.015	1.859	−0.001	21
0	4	4	49.380	−0.011	1.846	0.000	2
2	3	−4	52.870	−0.004	1.732	0.000	6
1	2	7	54.283	0.008	1.690	0.000	5
1	3	−7	54.990	0.012	1.670	0.000	5

^{a} $2\theta_{obs} - 2\theta_{calc}$.
^{b} $d_{obs} - d_{calc}$.

FIG. 1. UV/visible spectrum of $NaNb_2AsO_8$.

tal was selected and mounted on a thin glass fiber with cyanoacrylate adhesive, and room-temperature [25(2)°C] intensity data were collected on a Huber automated 4-circle diffractometer (graphite-monochromated Mo$K\alpha$ radiation, λ = 0.71073 Å) (27). After locating and centering 25 reflections (typical Ω-scan width $\approx$ 0.17°), the unit cell constants were optimized by least-squares refinement, resulting in the monoclinic lattice parameters of a = 4.8970(6) Å, b = 8.516(2)Å, c = 15.075(3)Å, and β = 98.971(6)°, (e.s.d. in parentheses). Intensity data were collected in the θ-2θ scanning mode with standard reflections monitored for intensity variation throughout the course of the experiment. The scan speed was 6°/min with a scan range of 1.3° below $K\alpha_1$ to 1.6° above $K\alpha_2$. No significant variation in standards was observed. The raw data were reduced using a Lehmann–Larsen profile-fitting routine (28) and the normal corrections for Lorentz and polarization effects were made. The systematic absences in the reduced data ($h0l$, h + l; $0k0$, k) uniquely indicated space group $P2_1/n$ (nonstandard setting of $P2_1/c$, No. 14). After data merging (3146 measured intensities; R_{Int} = 5.2%), 2121 reflections were considered observable according to the criterion $I > 3\sigma(I)$.

The crystal structure of NaNb₂AsO₈ was partially solved (Nb, As, some O-atom positions) using the direct-

TABLE 3
Atomic Positional Parameters for NaNb₂AsO₈

Atom	x	y	z	$U_{eq}{}^a$
Na(1)	0.0872(6)	−0.0198(3)	0.6202(2)	0.0337
Nb(1)	0.09300(7)	0.56984(4)	0.63908(2)	0.0177
Nb(2)	−0.47542(7)	0.70444(4)	0.48120(2)	0.0184
As(1)	−0.34186(9)	0.75995(5)	0.76487(3)	0.0180
O(1)	−0.0952(7)	0.7564(4)	0.7004(2)	0.0222
O(2)	0.4181(6)	0.6206(4)	0.7406(2)	0.0232
O(3)	−0.2607(6)	0.5418(4)	0.5624(2)	0.0203
O(4)	0.2539(7)	0.7151(4)	0.5660(2)	0.0213
O(5)	−0.0275(7)	0.4426(4)	0.7461(2)	0.0218
O(6)	0.2571(7)	0.3895(4)	0.6083(2)	0.0235
O(7)	−0.2800(7)	0.8737(4)	0.5056(2)	0.0247
O(8)	−0.7261(7)	0.7859(4)	0.3738(2)	0.0225

^{a} $U_{eq}(\text{Å}^2)$ = $1/3[U_{22} + 1/\sin^2\beta(U_{11} + U_{33} + 2U_{13}\cos\beta)]$.

TABLE 2
Crystallographic Parameters for NaNb₂AsO₈

Empirical formula	Nb₂As₁Na₁O₈
Formula weight	410.79
Habit	Gold needle
Crystal size (mm)	0.1 × 0.1 × 0.5
Crystal system	Monoclinic
a (Å)	4.8970(6)
b (Å)	8.516(2)
c (Å)	15.075(3)
β (°)	98.971(6)
V (Å³)	620.98
Z	4
Space group	$P2_1/n$ (No. 14)
T (°C)	25(2)
$\lambda(\text{Mo}K\alpha)$ (Å)	0.71073
ρ_{calc} (g/cm³)	4.39
$\mu(\text{Mo}K\alpha)$ (cm⁻¹)	88.8
Absorption correction	ψ-scan
hkl data range	−7→ 7, 0 → 12, 0 → 22
min, max $\Delta\rho$ (e/Å³)	−1.28, 1.69
Total data	3146 ($2\theta < 65°$)
Observed data^a	2121
Parameters	110
$R(F)^b$ (%)	5.31
$R_w(F)^c$ (%)	5.15
S (goodness of fit)	1.12

^{a} $I > 3\sigma(I)$ after merging.
^{b} R = $\Sigma| |F_o| - |F_c| |/\Sigma|F_o|$.
^{c} R_w = $[\Sigma w(|F_o| - |F_c|)^2/\Sigma w|F_o|^2]^{1/2}$.

methods program SHELXS-86 (29) and the other atom positions were located from Fourier difference maps during the refinement procedure. The final cycles of full-matrix least-squares refinement were against F and included anisotropic temperature factors and a secondary extinction correction, (30). Neutral-atom scattering factors, taking account of anomalous dispersion terms, were obtained from the "International Tables" (31). At the end of the refinement (R = 5.31%, R_w = 5.15%, Tukey–Prince weighting scheme (32)), analysis of the various trends in F_o versus F_c revealed no unusual effects. The least-squares, Fourier, and subsidiary calculations were performed using the Oxford CRYSTALS system (33), running on a DEC MicroVAX 3100 computer. Tables of anisotropic thermal factors and observed and calculated structure factors are available as supplementary material. Crystallographic and data-collection parameters for NaNb₂AsO₈ are summarized in Table 2.

CRYSTAL STRUCTURE

Final atomic positional and equivalent isotropic thermal parameters (34) for NaNb₂AsO₈ are listed in Table 3, with selected bond distance/angle data in Tables 4 and 5. The asymmetric unit, which consists of 1 Na, 2 Nb, 1 As, and 8 O atoms, and atom-labeling scheme for NaNb₂As O₈ is illustrated in Fig. 2.

The new crystal structure of NaNb₂AsO₈ consists of an edge- and vertex-linked three-dimensional network of Nb(1)O₆, Nb(2)O₅, and AsO₄ polyhedra, linked via Nb–O–Nb and Nb–O–As bonds. The Nb(1) polyhedron is a fairly distorted octahedron (d_{av}(Nb–O) = 1.995(2) Å, variation of cis O–Nb–O angles: 79.4(1)–99.3(1)°). The Nb(2) moiety (d_{av} = 1.952(2) Å) may be described as square-pyramidal (Fig. 2), although a very long contact to

TABLE 4
Bond Distances (Å) for NaNb$_2$AsO$_8$

Na(1)–O(1)	2.495(4)	Na(1)–O(2)	2.419(4)
Na(1)–O(4)	2.577(4)	Na(1)–O(5)	2.731(4)
Na(1)–O(7)	2.465(4)	Na(1)–O(7)'	2.568(4)
Na(1)–O(8)	2.675(4)		
Nb(1)–O(1)	2.120(3)	Nb(1)–O(2)	2.074(3)
Nb(1)–O(3)	1.941(3)	Nb(1)–O(4)	1.906(3)
Nb(1)–O(5)	2.103(3)	Nb(1)–O(6)	1.826(3)
Nb(2)–O(3)	2.030(3)	Nb(2)–O(4)	1.982(3)
Nb(2)–O(6)	2.013(3)	Nb(2)–O(7)	1.738(3)
Nb(2)–O(8)	1.997(3)	Nb(2)–O(3)'	2.494(3)^a
As(1)–O(1)	1.664(3)	As(1)–O(2)	1.670(3)
As(1)–O(5)	1.680(3)	As(1)–O(8)	1.697(3)

^{a} See text.

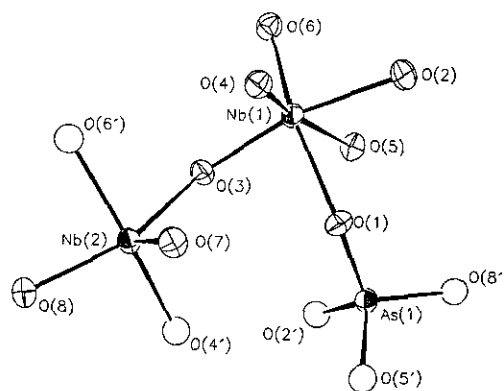**FIG. 2.** ORTEP (37) view of the asymmetric unit of NaNb$_2$AsO$_8$ (Na species omitted), showing the atomic connectivity and labeling scheme. Thermal ellipsoids are illustrated at the 50% level, with symmetry-equivalent atoms indicated by plain spheres with a radius equivalent to U_{eq} for those species.

O(3) ($d = 2.494(7)$ Å) would complete an extremely distorted octahedron (Fig. 3). The arsenate group is tetrahedral with a typical d_{av}(As–O) of 1.677(2) Å, although the O–As–O tetrahedral angles are quite distorted (min = 99.6(2)°, max = 114.2(2)°). Bond-valence sums (BVSs) for the Nb^V and As^V species, calculated using the Brown–Wu formalism (35), give the following values: BVS[Nb(1)] = 5.02; BVS[Nb(2)] = 4.70, or 4.96 if the ~2.5-Å bond to O(3) is included in the calculation; BVS[As(1)] = 5.10. The Nb–O and As–O bond distances in NaNb$_2$AsO$_8$ accord with the expected average separa-

tions for these species, based on ionic-radii sums (36): d_{calc}(Nb–O) = 1.99 Å and d_{calc}(As–O) = 1.68 Å.

Four oxygen atoms (O(1), O(2), O(5), and O(8)) partake in Nb–O–As bonds, with θ_{av} = 133.6(2)°. O(3), O(4), and O(6) form Nb(1)–O–Nb(2) links (θ_{av} = 135.7(2)°), and O(7) is part of a short "niobyl" Nb–O link, not linked to any other atom except the Na$^+$ cation. All the oxygen atoms except O(3) and O(6) also bond to the sodium cation. The sodium cation is seven-coordinate with respect to nearby ($d < 2.8$ Å) oxygen atoms, with d_{av}(Na–O) = 2.561(1) Å and a BVS of 1.00. The average ionic-radii-sum bond distance for seven-coordinate Na$^+$ is 2.47 Å, slightly shorter than the observed value. The sodium-atom coordination (Fig. 4) is irregular, but approximates a pentagonal bipyramid (apical oxygen atoms O(1) and O(7)').

TABLE 5
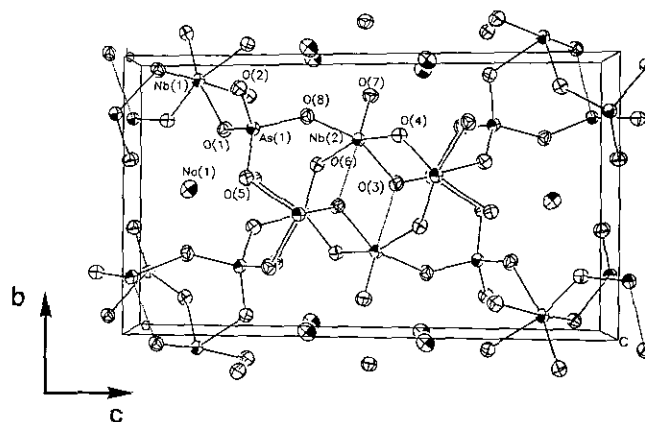### Bond Angles (°) for NaNb$_2$AsO$_8$

O(2)–Nb(1)–O(1)	81.8(1)	O(3)–Nb(1)–O(1)	86.8(1)
O(3)–Nb(1)–O(2)	167.3(1)	O(4)–Nb(1)–O(1)	90.7(1)
O(4)–Nb(1)–O(2)	87.3(1)	O(4)–Nb(1)–O(3)	98.4(1)
O(5)–Nb(1)–O(1)	81.9(1)	O(5)–Nb(1)–O(2)	79.4(1)
O(5)–Nb(1)–O(3)	93.6(1)	O(5)–Nb(1)–O(4)	165.5(1)
O(6)–Nb(1)–O(1)	168.3(1)	O(6)–Nb(1)–O(2)	92.6(1)
O(6)–Nb(1)–O(3)	97.6(1)	O(6)–Nb(1)–O(4)	99.3(1)
O(6)–Nb(1)–O(5)	87.1(1)		
O(4)–Nb(2)–O(3)	88.7(1)	O(6)–Nb(2)–O(3)	81.6(1)
O(6)–Nb(2)–O(4)	158.2(1)	O(7)–Nb(2)–O(3)	102.8(1)
O(7)–Nb(2)–O(4)	103.1(1)	O(7)–Nb(2)–O(6)	98.0(2)
O(8)–Nb(2)–O(3)	157.0(1)	O(8)–Nb(2)–O(4)	96.8(1)
O(8)–Nb(2)–O(6)	85.3(1)	O(8)–Nb(2)–O(7)	97.6(1)
O(2)–As(1)–O(1)	114.2(2)	O(5)–As(1)–O(1)	105.0(2)
O(5)–As(1)–O(2)	113.1(2)	O(8)–As(1)–O(1)	113.4(2)
O(8)–As(1)–O(2)	99.6(2)	O(8)–As(1)–O(5)	111.9(1)
As(1)–O(1)–Nb(1)	132.3(2)	As(1)–O(2)–Nb(1)	138.0(2)
Nb(2)–O(3)–Nb(1)	127.2(2)	Nb(2)–O(4)–Nb(1)	136.2(2)
As(1)–O(5)–Nb(1)	123.3(2)	Nb(2)–O(6)–Nb(1)	143.6(2)
As(1)–O(8)–Nb(2)	140.8(2)		

FIG. 3. The crystal structure of NaNb$_2$AsO$_8$, viewed down [100]. Selected atoms are labeled, and the "long" Nb(2)–O(3) bonds are illustrated by dotted lines. Fifty percent thermal ellipsoids; Na–O bonds omitted for clarity.
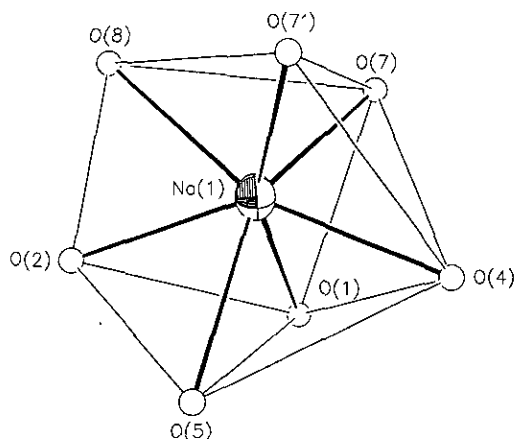
FIG. 4. Detail of the seven-fold sodium-atom coordination sphere in NaNb$_2$AsO$_8$. O atoms illustrated as spheres of arbitrary radius, with O $\cdots$ O nonbonding contacts of <4.0 Å shown as thin lines.

The polyhedral connectivity in NaNb$_2$AsO$_8$ leads to a structure containing columns of Nb(1)O$_6$/Nb(2)O$_5$ units (Fig. 5), crosslinked by AsO$_4$ groups, enclosing one-dimensional channels which propagate in the **a** direction (Fig. 3). These channels are large enough to be occupied by the sodium cations in "side-by-side" configuration, as the sodium–sodium distance (d = 3.608(6)Å) is big enough to allow simultaneous full occupancy of both sites in the channels, which may be contrasted with the disordered potassium channels in KNb$_4$AsO$_{13}$ (21).

CONCLUSIONS

The preparation, structure, and some properties of NaNb$_2$AsO$_8$ are described. This phase complements the many other M/Nb/(P, As)/O phases noted in the introduction and has similar polyhedral building blocks, but is
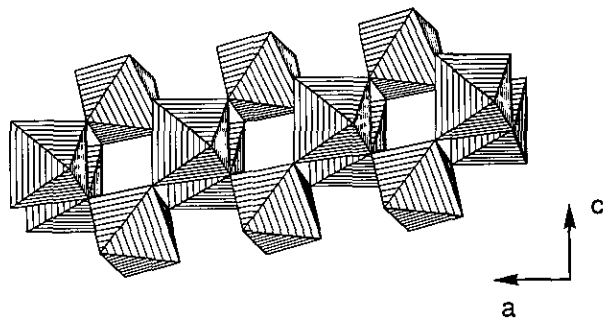

FIG. 5. Polyhedral STRUPLO (38) plot of the niobium/oxygen chain configuration in NaNb$_2$AsO$_8$, viewed approximately down the **b** direction. Pairs of "edge-sharing" Nb(2)-centered groups are linked into an infinite chain by pairs of Nb(1)O$_6$ groups. For plotting, the Nb(2) moiety has been assumed to be octahedral, incorporating the long Nb(2)–O(3) bond into its coordination sphere, to emphasize the "double chain" connectivity.

not isostructural with any of them. Its most interesting structural feature is the Nb(2)-centered unit, which is "intermediate" between octahedral and distorted square-pyramidal geometry and could perhaps be notated as an NbO$_{5+1}$ unit. Nb(2) is displaced from the plane formed by the oxygen atoms O(3), O(4), O(6), and O(8) by ~0.36Å, toward oxygen atoms O(7), resulting in the long Nb(2)–O(3)' bond (Table 4).

The three previously reported potassium niobium arsenate phases (20–22) do show some aspects of structural similarity, when compared with NaNb$_2$AsO$_8$. K$_2$Nb$_2$As$_2$O$_{11}$ (20) has an open structure, built up from NbO$_6$ and AsO$_4$ groups, linked via Nb–O–As and Nb–O–Nb vertices, enclosing the "guest" K-cations in one-dimensional channels, but with a quite different connectivity to that observed in NaNb$_2$AsO$_8$. Both of the crystallographically distinct NbO$_6$ groups in K$_2$Nb$_2$As$_2$O$_{11}$ are distorted (d_{min}(Nb–O) $\approx$ 1.73 Å, d_{max}(Nb–O) $\approx$ 2.23 Å), but not to the extent of Nb(2) in NaNb$_2$AsO$_8$.

In KNb$_4$AsO$_{13}$ (21), the NbO$_6$ and AsO$_4$ moieties are linked via Nb–O–As and Nb–O–Nb vertices, and also via edge-sharing between pairs of NbO$_6$ octahedra. Both distinct NbO$_6$ groups (d_{min}(Nb–O) $\approx$ 1.82 Å, d_{min}(Nb–O) $\approx$ 2.24 Å) show somewhat less distortion than that observed in K$_2$Nb$_2$As$_2$O$_{11}$. This polyhedral connectivity also leads to one-dimensional channels, of two types: one "6-ring" and one "8-ring." The potassium cations show twofold disorder in this larger channel.

K$_3$NbAs$_2$O$_9$ (22) is a layer structure, built up from the typical NbO$_6$ and AsO$_4$ polyhedral units, linked by vertices. The interlayer region is occupied by the potassium species. The NbO$_6$ unit is highly distorted (d_{min}(Nb–O) $\approx$ 1.75 Å, d_{max}(Nb–O) $\approx$ 2.32 Å), but again not to the extent observed for the Nb(2) octahedron in NaNb$_2$AsO$_8$. The authors considered the niobium-atom coordination in K$_3$NbAs$_2$O$_9$ to be definitely octahedral rather than square pyramidal.

In conclusion, NaNb$_2$AsO$_8$ is another new phase with a simple stoichiometry in this interesting area of solid-state chemistry. Its structure is completely different to its MNb$_2$PO$_8$-type phosphate analogues, such as K$_{2/3}$Li$_{1/3}$Nb$_2$PO$_8$ (5). NaNb$_2$AsO$_8$ contains an isolated, short, Nb–O bond, which might be expected to have very favorable optical properties due to the highly polarizable nature of this bond (3). Although the crystal structure of NaNb$_2$AsO$_8$ is centrosymmetric, and the question of SHG-response does not arise in this case, we are continuing our explorations of the M/Nb/(As, P)/O phase space in an effort to prepare other new phases which may have practical applications in optical physics.

ACKNOWLEDGMENTS

REFERENCES

1. J. D. Bierlein and H. Vanherzeele, *J. Opt. Soc. Am. B* **6,** 622 (1989).
2. G. D. Stucky, M. L. F. Phillips, and T. E. Gier, *Chem. Mater.* **1,** 492 (1989).
3. J. G. Bergmann and G. R. Crane, *J. Solid State Chem.* **12,** 172 (1975).
4. M. Munowitz, R. H. Jarman, and J. F. Harrison, *Chem. Mater.* **4,** 1296 (1992).
5. G. Costentin, M. M. Borel, A. Grandin, A. Leclaire, and B. Raveau, *J. Solid State Chem.* **90,** 279 (1991).
6. C. S. Liang, W. T. A. Harrison, M. M. Eddy, T. E. Gier, and G. D. Stucky, *Chem. Mater.* **5,** 917 (1993).
7. W. T. A. Harrison, C. S. Liang, J. M. Nicol, and G. D. Stucky, *Z. Kristallogr.* (1994), in press.
8. SHG data for polycrystalline β-BaB$_2$O$_4$ supplied by J. D. Bierlein, Central Research and Development Laboratory, E. I. du Pont de Nemours, Wilmington, DE.
9. M. El Brahimi and J. Durand, *Rev. Chim. Miner.* **23,** 146 (1986).
10. V. P. Nikolaev, G. G. Sadikov, A. V. Lavrov, and M. A. Porai-Koshits, *Dokl. Akad. Nauk SSSR* **264,** 859 (1982).
11. S. A. Linde, Y. E. Gorbunova, A. V. Lavrov, and I. V. Tananaev, *Dokl. Akad. Nauk SSSR* **250,** 96 (1980).
12. A. Leclaire, M. M. Borel, A. Grandin, and B. Raveau, *J. Solid State Chem.* **80,** 12 (1989).
13. A. Leclaire, A. Benabbas, M. M. Borel, A. Grandin, and B. Raveau, *J. Solid State Chem.* **83,** 245 (1989).
14. A. Benabbas, M. M. Borel, A. Grandin, A. Leclaire, and B. Raveau, *J. Solid State Chem.* **84,** 365 (1990).
15. A. Benabbas, M. M. Borel, A. Grandin, A. Leclaire, and B. Raveau, *J. Solid State Chem.* **89,** 75 (1990).
16. A. Benabbas, M. M. Borel, A. Grandin, A. Leclaire, and B. Raveau, *J. Solid State Chem.* **87,** 360 (1990).
17. M. M. Borel, A. Grandin, G. Costentin, A. Leclaire, and B. Raveau, *Mater. Res. Bull.* **25,** 1155 (1990).
18. M. M. Borel, A. Benabbas, H. Rebbah, A. Grandin, A. Leclaire, and B. Raveau, *Eur. J. Solid State Inorg. Chem.* **27,** 525 (1990).
19. A. Benabbas, M. M. Borel, A. Grandin, J. Chardon, A. Leclaire, and B. Raveau, *J. Solid State Chem.* **91,** 323 (1991).
20. A. Benabbas, M. M. Borel, A. Grandin, A. Leclaire, and B. Raveau, *J. Solid State Chem.* **92,** 51 (1991).
21. A. Leclaire, M. M. Borel, A. Grandin, and B. Raveau, *Mater. Res. Bull.* **26,** 207 (1991).
22. M. F. Zid, T. Jouini, N. Jouini, and M. Omezzine, *J. Solid State Chem.* **74,** 337 (1988).
23. A. Heddard, T. Jouini, Y. Piffard, and N. Jouini, *J. Solid State Chem.* **77,** 293 (1988).
24. M. F. Zid, T. Jouini, N. Jouini, and M. Omezzine, *J. Solid State Chem.* **82,** 14 (1989).
25. K. Yvon, W. Jeitscho, and E. Parthe, *J. Appl. Crystallogr.* **10,** 73 (1977).
26. E. J. Baran, J. C. Pedregosa, and P. J. Aymonino, *J. Mol. Spectrosc.* **22,** 377 (1974).
27. Data collection and reduction were controlled using a locally modified version of the UCLA Crystallographic Computing Package, developed by C. E. Strouse, Department of Chemistry, UCLA, Los Angeles, CA.
28. M. S. Lehmann and F. K. Larsen, *Acta Crystallogr. Ser. A* **30,** 580 (1974).
29. G. M. Sheldrick, "SHELXS-86 User Guide," Crystallography Department, University of Göttingen, Germany, 1986.
30. A. C. Larson, *Acta Crystallogr.* **23,** 664 (1967).
31. "International Tables for X-Ray Crystallography," Vol. IV, Kynoch Press, Birmingham (1974).
32. J. R. Carruthers and D. J. Watkin, *Acta Crystallogr. Ser. A* **35,** 698 (1979).
33. D. J. Watkin, J. R. Carruthers, and P. W. Betteridge, "CRYSTALS User Guide," Chemical Crystallography Laboratory, Oxford University, UK (1985).
34. R. X. Fischer and E. Tillmanns, *Acta Crystallogr. Ser. C* **44,** 775 (1988).
35. I. D. Brown and K. K. Wu, *Acta Crystallogr. Ser. B* **32,** 1957 (1975).
36. R. D. Shannon, *Acta Crystallogr. Ser. A* **32,** 751 (1976).
37. C. K. Johnson, Oak Ridge National Laboratory Report ORNL-5138, Oak Ridge, TN, 1976, with local modifications.
38. R. X. Fischer, *J. Appl. Crystallogr.* **18,** 258 (1985).